Targeting CD19-positive lymphomas with the antibody-drug conjugate loncastuximab tesirine: preclinical evidence of activity as a single agent and in combination therapy

Chiara Tarantelli,[1*] David Wald,[2*] Nicolas Munz,[1] Filippo Spriano,[1] Alessio Bruscaggin,[1] Eleonora Cannas,[1] Luciano Cascione,[1,3] Eugenio Gaudio,[1] Alberto J. Arribas,[1,3] Shivaprasad Manjappa,[4] Gaetanina Golino,[1] Lorenzo Scalise,[1] Maria Teresa Cacciapuoti,[5] Emanuele Zucca,[1,6] Anastasios Stathis,[6,7] Giorgio Inghirami,[5] Patrick H. van Berkel,[8] Davide Rossi,[1,6] Paolo F. Caimi,[9] Francesca Zammarchi[8] and Francesco Bertoni[1,6]

[1]Institute of Oncology Research, Faculty of Biomedical Sciences, USI, Bellinzona, Switzerland; [2]Case Western Reserve University, Cleveland, OH, USA; [3]SIB Swiss Institute of Bioinformatics, Lausanne, Switzerland; [4]Fred Hutchinson Cancer Center, Seattle, WA, USA; [5]Department of Pathology and Laboratory Medicine, Weill Cornell Medicine, New York, NY, USA; [6]Oncology Institute of Southern Switzerland, Ente Ospedaliero Cantonale, Bellinzona, Switzerland; [7]Faculty of Biomedical Sciences, USI, Lugano, Switzerland; [8]ADC Therapeutics (UK) Ltd., London, UK and [9]Cleveland Clinic/Case Comprehensive Cancer Center, Cleveland, OH, USA

*CT and DW contributed equally as first authors.

Correspondence: C. Tarantelli
chiara.tarantelli@ior.usi.ch

F. Bertoni
francesco.bertoni@ior.usi.ch

Received: August 29, 2023.
Accepted: May 2, 2024.
Early view: May 9, 2024.

https://doi.org/10.3324/haematol.2023.284197

Abstract

Antibody-drug conjugates (ADC) represent one of the most successful therapeutic approaches introduced into clinical practice in the last few years. Loncastuximab tesirine (ADCT-402) is a CD19-targeting ADC in which the antibody is conjugated through a protease cleavable dipeptide linker to a pyrrolobenzodiazepine dimer warhead (SG3199). Based on the results of a phase II study, loncastuximab tesirine was recently approved for adult patients with relapsed/refractory large B-cell lymphoma. We assessed the activity of loncastuximab tesirine using *in vitro* and *in vivo* models of lymphomas, correlated its activity with levels of CD19 expression, and identified combination partners providing synergy with the ADC. Loncastuximab tesirine was tested across 60 lymphoma cell lines. It had strong cytotoxic activity in B-cell lymphoma cell lines. The *in vitro* activity was correlated with the level of CD19 expression and intrinsic sensitivity of cell lines to the ADC's warhead. Loncastuximab tesirine was more potent than other anti-CD19 ADC (coltuximab ravtansine, huB4-DGN462), although the pattern of activity across cell lines was correlated. The activity of loncastuximab tesirine was also largely correlated with cell line sensitivity to R-CHOP. Combinatorial *in vitro* and *in vivo* experiments identified the benefit of adding loncastuximab tesirine to other agents, especially BCL2 and PI3K inhibitors. Our data support the further development of loncastuximab tesirine for use as a single agent and in combination for patients affected by mature B-cell neoplasms. The results also highlight the importance of CD19 expression and the existence of lymphoma populations characterized by resistance to multiple therapies.

Introduction

Despite recent improvements, current therapies are not yet curative for too many patients affected by lymphoid neoplasms,[1-3] and novel therapeutic strategies are still needed. Antibody-drug conjugates (ADC) represent one of the most successful therapeutic approaches introduced into clinical practice in the last 25 years.[4,5] ADC are complex compounds that contain three components: an antibody, a warhead (i.e., a cytotoxic agent), and a linker that joins the two together. ADC enable targeted delivery of potent warheads into tumor cells using antibodies against tumor antigens.

Due to its pattern of expression and its biological role in lymphocytes, the B-cell marker CD19 has been heavily exploited for antibody-based therapies, including ADC, and, more recently, for cellular therapies.[4,6-10] Loncastuximab tesirine (ADCT-402) is a CD19-targeting ADC, in which the CD19-specific antibody is stochastically conjugated through a protease cleavable dipeptide linker to a pyrrolobenzodiazepine (PBD) dimer warhead (SG3199).[11] Following binding to CD19-positive cells, loncastuximab tesirine is rapidly internalized and transported to lysosomes, where the linker is cleaved to release the PBD dimer SG3199.[11] In contrast to the microtubule-disrupting monomethyl auristatin E (MMAE) used in the CD30-targeting brentuximab vedotin and the CD79B-targeting polatuzumab vedotin ADC,[12,13] SG3199 belongs to a new generation of DNA cross-linking agents. It binds to guanine residues in the DNA minor groove, forming covalent cross-links of the two DNA strands.[14,15] Loncastuximab tesirine has been studied in various clinical trials[16-18] and, based on the results of a phase II study,[16,19] it was recently approved in the USA and Europe for the treatment of adult patients with relapsed/refractory (R/R) large B-cell lymphoma after at least two prior lines of systemic therapy.[20]

Here, we assessed the anti-tumor activity of loncastuximab tesirine in a large panel of lymphoma cell lines, with a focus on the expression of its target and the identification of active combination partners.

Methods

Details on the cell lines and compounds used in this study, together with information on the Ly4.0 cancer personalized profiling (CAPP)-sequencing genomic DNA assay and variant calling are provided in the *Online Supplementary Materials and Methods*. The full methods for the immunoblotting, and cell cycle analysis as well as the data mining are also described in the *Online Supplementary Materials and Methods*.

In vitro cytotoxic activity

The cytotoxic activity of loncastuximab tesirine was assessed *in vitro*, as previously described.[21] Briefly, cells were exposed to each compound for 96 hours and assayed by MTT (3-[4,5-dimethylthiazolyl-2]-2, 5-diphenyltetrazolium-bromide). For R-CHOP treatment, cells were exposed for 72 hours to 1 μg/mL CHOP + 100 μg/mL rituximab at five different concentrations in 1:10 serial dilutions. Rituximab was diluted to clinically recommended serum levels[22] and CHOP represented a mix reflecting the clinical ratios of the drugs[23,24] (85%, 4-hydroperoxy-cyclophosphamide; 5.5%, doxorubicin; 0.16%, vincristine; 11.1%, prednisolone). Cells were also exposed in parallel to the PBD dimer SG3199 and the isotype-control ADC B12-SG3249.[25]

Synergism was assessed by exposing cells for 96 hours to increasing doses of loncastuximab tesirine and each of the other agents, either alone or in combination, followed by an MTT assay. The Chou-Talalay combination index (CTI) was determined as previously described.[26] Combinations were defined as synergistic (median CTI <0.9), additive (median CTI, 0.9-1.1), or of no benefit/antagonist (median CTI >1.1).

CD19 expression

Absolute cell surface CD19 expression was determined via quantification of the antigen on the surface of lymphoma cell lines using Quantum Simply Cellular anti-human IgG beads (Bangs Laboratories) to create a calibration curve. Antibody-binding capacity values were then normalized to those of the control isotype antibody B12.

CD19 RNA expression values were extracted from the datasets GSE94669, previously obtained using a targeted RNA-sequencing approach (HTG EdgeSeq Oncology Biomarker panel) and microarray-based technology (Illumina HT-12 arrays),[26] and GSE221770, previously produced via total RNA sequencing.[27]

Patient-derived xenograft cell line

A patient-derived xenograft was produced in the context of protocols approved by Cornell University (Institutional Review Board: 107004999, 0201005295, and 1410015560; Universal consent: 1302013582; *in vivo* protocol 2014-0024). Full methods are provided in the *Online Supplementary Materials and Methods*.

In vivo experiments

Mice maintenance and animal experiments were performed under the institutional guidelines established for the Animal Facility at The Institute of Research in Biomedicine (license number TI 49-2018) (TMD8 experiment) or following the policies and regulations set out by the Institutional Animal Care and Use Committee of Case Western Reserve University (JEKO1 experiment). Full methods are provided in the *Online Supplementary Materials and Methods*.

Results

Loncastuximab tesirine has strong cytotoxic activity in B-cell lymphoma cell lines

Loncastuximab tesirine was tested for its antiproliferative activity across 60 lymphoma cell lines, which were exposed to the ADC for 96 hours (*Online Supplementary Table S2*). Loncastuximab tesirine had activity in the picomolar range, with a median half-maximal inhibitory concentration (IC_{50}) of 4.1 pM (95% confidence interval: [95% CI]:, 2-9.6 pM) among 48 lymphoma cell lines derived from mature B-cell lymphomas. Conversely, the antiproliferative activity of loncastuximab tesirine was over 800-fold lower in nine T-cell lymphoma cell lines (median IC_{50} 3.5 nM; 95%

CI: 0.8-11 nM; *P*<0.0001) (*Online Supplementary Figure S1*). The activity was similar among all the individual B-cell lymphoma subtypes except Hodgkin lymphoma models, which were over 600-fold less sensitive to loncastuximab tesirine than were the other cell lines (*P*=0.009) (Table 1). Loncastuximab tesirine exerted its antilymphoma activity via induction of apoptosis, as shown in two exemplar cell lines derived from activated B-cell (ABC) DLBCL (TMD8 cell line) or germinal center B-cell (GCB) DLBCL (VAL cell line) (*Online Supplementary Figure S2*).

The sensitivity to loncastuximab tesirine did not differ between DLBCL cell lines with (N=15) and without (N=11) *BCL2* translocation or with (N=16) and without (N=7) *TP53* inactivation. Instead, DLBCL cell lines with *MYC* translocation (N=10) *versus* cell lines without the translocation (N=16) and DLBCL cell lines with (N=7) *versus* those without (N=19) concomitant *BCL2* and *MYC* translocation (double hit) had lower IC_{50} values (both comparisons, *P*<0.05) (*Online Supplementary Figure S3*).

The sensitivity to loncastuximab tesirine was also correlated with mutational status determined by targeted DNA sequencing designed to cover various coding genomic regions recurrently mutated in mature B-cell neoplasms (*Online Supplementary Table S4*). After multiple corrections, no somatic mutation was significantly associated with response to loncastuximab tesirine.

In parallel, we exposed the cells to an isotype-control ADC (B12-SG3249), which was active in the nanomolar range with no difference between B- and T-cell lymphoma cell lines: median IC_{50} values were 0.9 nM (95% CI: 0.7-2.2 nM) and 1.7 nM (95% CI: 0.8-12 nM), respectively.

Finally, loncastuximab tesirine was tested in three non-human lymphoma cell lines: IC_{50} values were 2 nM and 500 pM in two mouse cell lines and 175 pM in a canine DLBCL cell line, similar to what was achieved using the isotype-control ADC B12-SG3249, indicating a non-cross species anti-lymphoma activity not driven by CD19 targeting (*Online Supplementary Table S2*).

CD19 levels correlate with the cytotoxic activity of loncastuximab tesirine

We then focused on cell lines derived from mature B-cell lymphomas to assess whether CD19 cell surface expression levels correlated with the antitumor activity of loncastuximab tesirine. We measured the absolute CD19 surface expression levels on each cell line (*Online Supplementary Table S2*), and we used additional protein and RNA expression data we had previously obtained on the same panel of cell lines.[27,28] We observed that the CD19 expression levels associated with loncastuximab tesirine activity, as demonstrated by the negative correlation between IC_{50} values and CD19 expression values measured both at the cell surface protein level [(absolute quantitation, N=46, r=-0.44, *P*=0.002; relative quantitation, N=45, r=-0.4, *P*=0.006]) and RNA level [(microarrays, N=53, r=-0.74, *P*<0.0001; HTG, N=36, r=-0.5, *P*=0.002; RNA sequencing, N=44, r=-0.55, *P*<0.0001] (Figure 1A-E).

Based on the association mentioned above between the presence of *MYC* translocation and loncastuximab tesirine lower IC_{50} values (i.e., greater sensitivity), we explored the possible relationships between CD19 and *MYC* expression levels in DLBCL cells. Neither CD19 surface protein expression levels nor CD19 RNA levels differed between cell lines with or without *MYC* translocation (as a single genetic event or together with *BCL2* translocation) (*Online Supplementary Figure S4A-C*). Similarly, CD19 and *MYC* levels were not correlated (*Online Supplementary Figure S4D, E*). Finally, *MYC* RNA levels were negatively correlated with loncastuximab tesirine IC_{50} values (R=-0.35) but without reaching a statistical significance (*P*=0.089) (*Online Supplementary Figure S4F*).

The cytotoxic activity of loncastuximab tesirine's warhead SG3199 is not affected by the lymphoma subtype but differs based on the presence of genetic lesions

All cell lines were exposed to loncastuximab tesirine's warhead SG3199 (*Online Supplementary Table S2*). The median IC_{50} value was 0.85 pM (95% CI: 0.69-1.14) across

Table 1. Antitumor activity of loncastuximab tesirine in lymphoma cell lines.

	N of cell lines	Median IC_{50}, pM	95% confidence interval, pM
ABC DLBCL	7	35	7.3-880
GCB DLBCL	19	2	1.17-10.6
Mantle cell lymphoma	10	1.75	1.1-5.4
Marginal zone lymphoma	6	2.5	0.47-496
Chronic lymphocytic leukemia	2	15.75	5.5-26*
Hodgkin lymphoma	3	2750	600-14,000*
PMBCL	1	1.5	ND
Anaplastic large cell lymphoma	4	4875	700-11,500*
Cutaneous T-cell lymphoma	4	2500	900-35,000*
PTCL-NOS	1	850	ND

Half maximal inhibitory (IC_{50}) values were obtained after 96 hours of treatment. *The upper confidence limit was held at a maximum for the sample. ABC: activated B cell; DLBCL: diffuse large B-cell lymphoma; GCB: germinal center B cell; PMBCL: primary mediastinal large B-cell lymphoma; PTCL-NOS: peripheral T-cell lymphoma - not otherwise specified; ND: not determined.

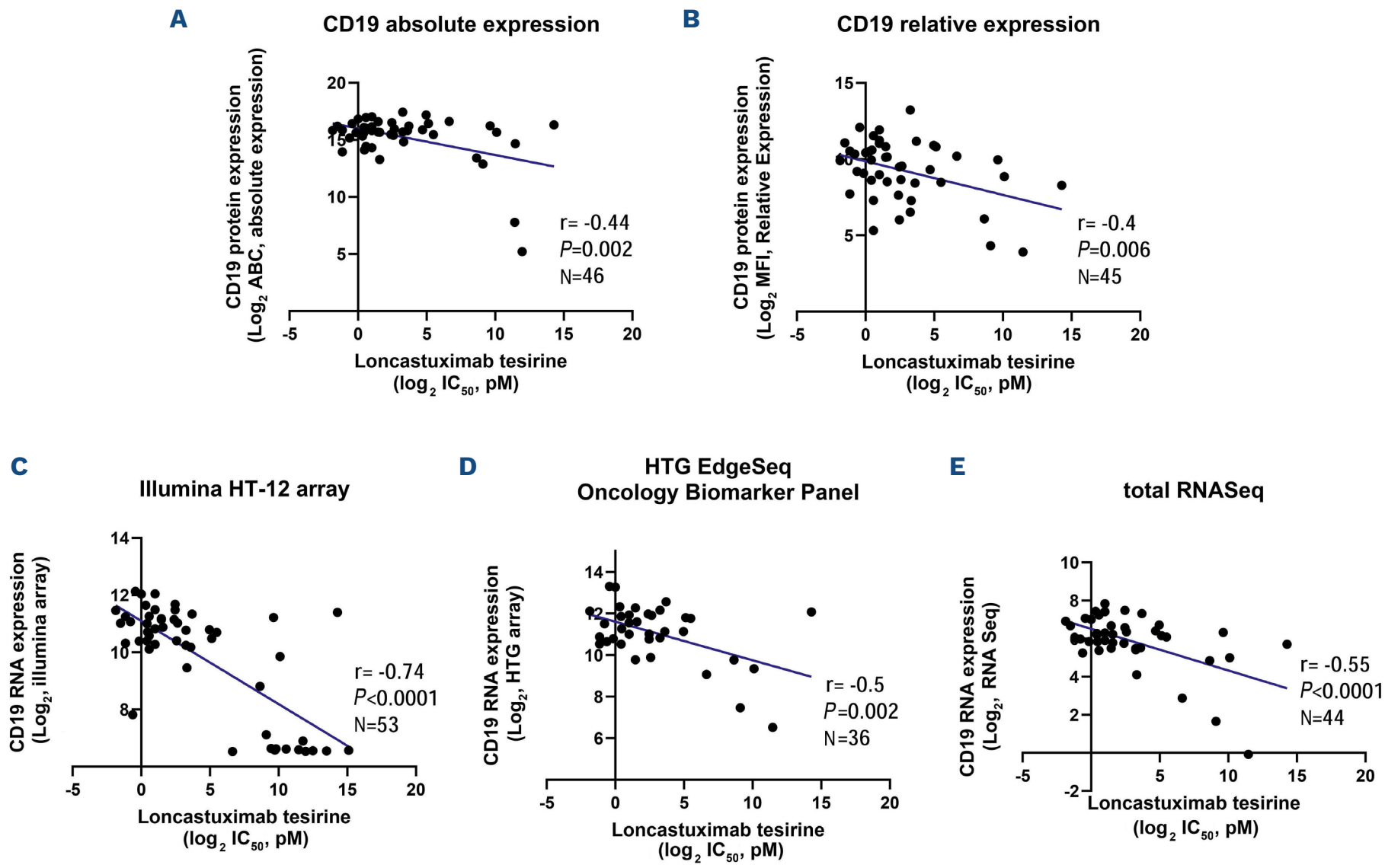

Figure 1. The *in vitro* antiproliferative activity of loncastuximab tesirine is correlated with CD19 expression. (A, B) Pearson correlations between loncastuximab tesirine activity and CD19 protein absolute expression (A) and relative expression (B). (C-E) Pearson correlations between loncastuximab tesirine's activity and CD19 transcripts measured with Illumina HT-12 arrays (C), the HTG biomarker panel (D), and total RNA sequencing data (E). ABC: antibody-binding capacity; IC_{50}: half maximal inhibitory concentration; MFI: mean fluorescence intensity.

all 60 lymphoma cell lines. Unlike what had been observed with loncastuximab tesirine, the activity of SG3199 did not differ between B- and T-cell lymphomas (Table 2, *Online Supplementary Figure S5*), and there was no correlation between the SG3199 IC_{50} values and CD19 expression values (*Online Supplementary Figure S6*). SG3199 was more potent than the ADC. The differences in terms of IC_{50} values between SG3199 and loncastuximab tesirine were statistically significant both considering all cell lines (P<0.0001) and considering only cell lines derived from B-cell lymphomas (P<0.0001) (*Online Supplementary Figure S7*).

The sensitivity to SG3199 appeared reduced in DLBCL cell lines with *TP53* inactivation when compared to *TP53* wild-type cell lines (P<0.001) (*Online Supplementary Figure S8A*). The *BCL2* translocation *per se* did not affect sensitivity to SG3199 (*Online Supplementary Figure S8B*). SG3199, like loncastuximab tesirine, was more active in DLBCL bearing *MYC* translocation as a single event or concomitant with *BCL2* translocation (P<0.05) (*Online Supplementary Figure S8C-D*). No correlation was observed between sensitivity to SG3199 and *MYC* RNA levels (*Online Supplementary Figure S9*).

The cytotoxic activities of loncastuximab tesirine and its warhead SG3199 are strongly correlated

The cytotoxic activity of loncastuximab tesirine and its warhead were strongly, positively correlated among all the cell lines (r=0.60, P<0.0001) and within the cell lines derived from mature B-cell lymphomas (r=0.63, P<0.0001) (Figure 2). Most of the cell lines that were less sensitive to the ADC (IC_{50} values higher than the 75th percentile, i.e., 768 pM) but sensitive to SG3199 (IC_{50} values lower than the 75th percentile, i.e., 2.9 pM) were the CD19-negative models (T-cell lymphomas, Hodgkin lymphoma) and the non-human lymphomas. Some cell lines, such as the splenic marginal zone lymphoma VL51, were highly sensitive to the warhead, but due to low CD19 expression had a high loncastuximab tesirine IC_{50} (VL51 IC_{50} >100 fold the median IC_{50} of the B-cell lymphoma cell lines). There were a few cell lines, especially the mantle cell lymphoma (MCL) REC1 and the DLBCL Pfeiffer and U2932, which had IC_{50} values higher than the 75th percentile for both loncastuximab tesirine and the SG3199 warhead, suggestive of primary resistance to the warhead. The GCB DLBCL cell line SU-

Table 2. Antitumor activity of the SG3199 warhead in lymphoma cell lines.

	N of cell lines	Median IC_{50}, pM	95% confidence interval, pM
ABC DLBCL	7	1.17	0.63-7.85
GCB DLBCL	19	1.14	0.75-1.53
Mantle cell lymphoma	10	0.53	0.53-1.66
Marginal zone lymphoma	6	0.53	0.53-0.85
Chronic lymphocytic leukemia	2	0.83	0.53-1.14*
Hodgkin lymphoma	3	4.97	0.85-29.24*
PMBCL	1	0.56	ND
Anaplastic large cell lymphoma	4	2.34	0.85-17.54*
Cutaneous T-cell lymphoma	4	1.59	0.53-23.39*
PTCL-NOS	1	0.53	ND

Half maximal inhibitory (IC_{50}) values were obtained after 96 hours of treatment. *The upper confidence limit was held at a maximum for the sample. ABC: activated B cell; DLBCL: diffuse large B-cell lymphoma; GCB: germinal center B cell; PMBCL: primary mediastinal large B-cell lymphoma; PTCL-NOS: peripheral T-cell lymphoma - not otherwise specified; ND: not determined.

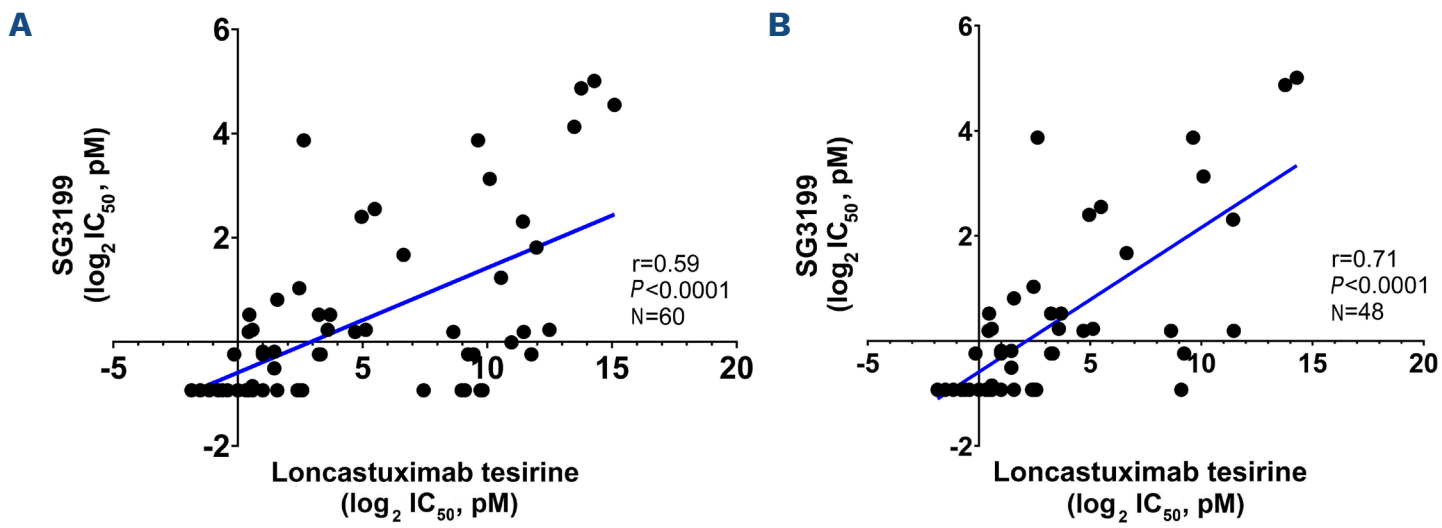

Figure 2. Correlation between the activity of loncastuximab tesirine and that of its warhead SG3199. (A, B) Pearson correlations between the half maximal inhibitory concentrations for loncastuximab tesirine and SG3199 across all cell lines (A) and in cell lines derived from B-cell lymphomas and Hodgkin lymphoma (B). IC_{50}: half maximal inhibitory concentration.

DHL-6 was sensitive to loncastuximab tesirine but resistant to its warhead SG3199. We confirmed that the antitumor activity was driven by the activity of the antibody itself rather than by the antibody complexed to the toxin (*Online Supplementary Figure S10*).

The cytotoxic activity of loncastuximab tesirine is correlated with the cytotoxicity of other CD19-targeting antibody-drug conjugates

We exploited data previously produced in our laboratory on the same panel of cell lines with two CD19-targeting ADC, coltuximab ravtansine (SAR3419), comprising the maytansinoid microtubule disruptor DM4, and huB4-DGN462, incorporating a DNA-alkylating payload.[28] The pattern of activity of loncastuximab tesirine correlated with those of both coltuximab ravtansine (r=0.38, *P*=0.01) and huB4-DGN462 (r=0.6, *P*<0.0001) (*Online Supplementary Figure S11*). Loncastuximab tesirine was more potent than both huB4-DGN462 (*P*=0.034) and coltuximab ravtansine (*P*<0.0001), although the exposure time previously used for the two additional ADC was shorter (72 *vs*. 96 hours). REC1, Pfeiffer, and U2932, the cell lines most resistant to loncastuximab tesirine, were also resistant to huB4-DGN462 and coltuximab ravtansine.

The pattern of cytotoxic activity of loncastuximab tesirine and R-CHOP are correlated

We exposed DLBCL cell lines (n=26) to the *in vitro* equivalent of R-CHOP (rituximab, cyclophosphamide, doxorubicin, vincristine, and prednisone) (*Online Supplementary Table S3*). The IC_{50} values obtained with R-CHOP correlated with the IC_{50} values of both loncastuximab tesirine (r=0.655, *P*<0.001) and SG3199 (r=0.425, *P*=0.03) (Figure 3). Some cell lines had a reduced sensitivity to R-CHOP (IC_{50} values higher than the 75th percentile, i.e., 0.077 μg/mL) but were very sensitive to loncastuximab tesirine and its warhead. A few cell lines (Pfeiffer, U2932, SU-DHL-16, SU-DHL-2) were less sensitive to loncastuximab tesirine and R-CHOP.

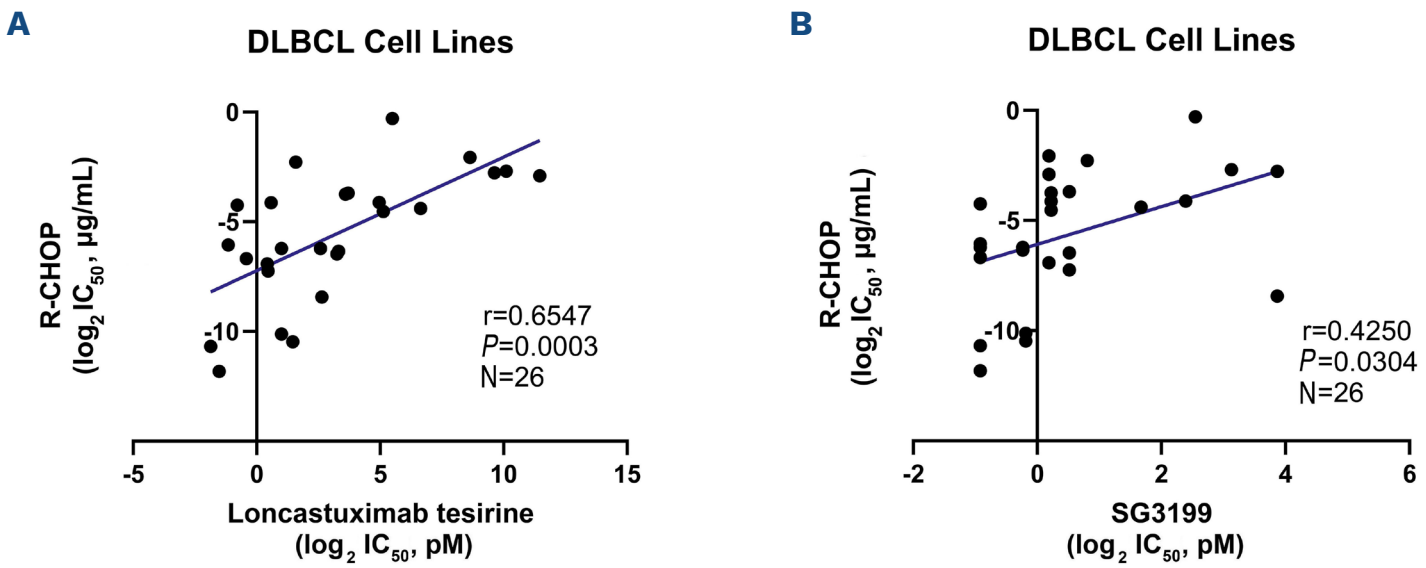

Figure 3. Correlation between the activity of loncastuximab tesirine or its warhead SG3199 and R-CHOP in diffuse large B-cell lymphoma cell lines. (A, B) Pearson correlations between the half maximal inhibitory concentrations values for R-CHOP and loncastuximab tesirine (A) or SG3199 (B). DLBCL: diffuse large B-cell lymphoma; R-CHOP: rituximab, cyclophosphamide, doxorubicin, vincristine, prednisone; IC_{50}: half maximal inhibitory concentration.

Loncastuximab tesirine is active in lymphoma cells following chimeric antigen receptor T-cell therapy

We took advantage of patient-derived xenograft cells from a patient treated with CD19-targeting chimeric antigen receptor (CAR) T cells (SS POST CAR19) to investigate a novel potential clinical application of loncastuximab tesirine. Cells expressed surface CD19 at a 26.72-fold level normalized to isotype (*Online Supplementary Figure S14*). The antiproliferative activity of loncastuximab tesirine (IC_{50}=0.7 nM) was superior to that of the naked antibody rB4v1.2 or the isotype associated with toxin B12-C220-SG3249 (IC_{50} values of 17.8 nM and not reached because the IC_{50} was beyond the tested range, respectively). The sensitivity to loncastuximab tesirine was below the 75th percentile in cell lines. Cells were still sensitive to the toxin (IC_{50}=0.37 pM).

Loncastuximab tesirine-based combinations appear beneficial *in vitro*

We explored the potential benefit of combining loncastuximab tesirine with drugs having an established role in treating lymphoma patients. We tested these combinations in two GCB DLBCL cell lines (VAL and WSU-DLCL2), two ABC DLBCL cell lines (TMD8 and OCI-LY-3) and two MCL lines (JEKO1 and JVM2). The combination partners were the BCL2 inhibitor venetoclax, the PI3Kδ inhibitor idelalisib, the PIK3α/δ inhibitor copanlisib, the anti-CD20 monoclonal antibody rituximab, the chemotherapy agent bendamustine, and the PARP inhibitor olaparib (Table 3). The combinations of loncastuximab tesirine with the proteasome inhibitor bortezomib, the BTK inhibitor ibrutinib, and the immunomodulator lenalidomide, were only tested on the ABC DLBCL cell lines, as these drugs are only used for the treatment of ABC DLBCL.

In DLBCL, the most beneficial combinations were loncastuximab tesirine plus venetoclax or idelalisib, with synergism achieved in all the models tested, followed by the combinations of the ADC plus bendamustine, copanlisib or olaparib. Synergism was also observed in one (OCI-Ly-3) of the two ABC DLBCL cell lines tested with loncastuximab tesirine plus ibrutinib. Combination with rituximab was synergistic in one cell line (VAL). No advantage was seen in combining loncastuximab tesirine with bortezomib or lenalidomide. In MCL, the most beneficial combinations were observed with venetoclax and copanlisib, with synergism in two out of two cell lines. The addition of idelalisib was synergistic in only one cell line (JVM2).

The effect on the cell cycle was investigated in four DLBCL cell lines (TMD8, OCI-LY-3, VAL, and WSU-DLCL2) treated with loncastuximab tesirine and the most promising targeted agents, i.e., venetoclax, idelalisib and copanlisib, as single agents and in combination, after 96 hours of treatment. In all the DLBCL cell lines, the increase of cells in sub-G1, compatible with cell death, was higher than in control in cells treated with loncastuximab tesirine either as a single agent or in combination (*Online Supplementary Figure S12*). Treatment with venetoclax, idelalisib, and copanlisib as single agents also increased the proportion of cells in the sub-G1 phase in WSU-DLCL2 and VAL and OCI-LY-3. In TMD8, an increase in sub-G1 was observed only with copanlisib as a single agent.

To understand the mechanism underlying the benefit given by loncastuximab tesirine when combined with venetoclax, idelalisib, or copanlisib, specific signaling pathways were explored by immunoblotting in TMD8 (ABC DLBCL) and WSU-DLCL2 (GCB DLBCL) cell lines (Figure 4, *Online Supplementary Figure S13*). CD19 downregulation was observed in both cell lines 24 hours after treatment with loncastuximab tesirine alone, and the downregulation increased further when loncastuximab tesirine was combined with each of the three drugs. The levels of pAKT were reduced in cells treated with the PI3K inhibitors idelalisib and copanlisib as single agents

or in combination with loncastuximab tesirine (Figure 4, *Online Supplementary Figure S13*). The levels of the anti-apoptotic protein MCL1 were downregulated by treatment with loncastuximab tesirine in the TMD8 cell line, and the effect was maintained when the combinations were used. In the WSU-DLCL2 cell line, MCL1 levels were also downregulated in cells treated with loncastuximab tesirine and with the PI3K inhibitors as single agents and in combination. In both cell lines, exposure to venetoclax upregulated MCL1, which was reduced in combination with loncastuximab tesirine. Cleaved PARP1, a marker of apoptosis, was slightly increased when loncastuximab tesirine was combined with the other three drugs.

Loncastuximab tesirine-based combinations are beneficial *in vivo*

An ABC DLBCL xenograft (TMD8 cell line) was used to validate the combination of loncastuximab tesirine with copanlisib *in vivo*. We first evaluated both compounds as single agents to define the doses to be combined. Mice (N=5 per group) bearing subcutaneous (sc) TMD8 xenografts were treated with control (phosphate-buffered saline, administered intravenously [iv]), three different doses of loncastuximab tesirine (0.1 mg/kg *vs*. 0.3 mg/kg *vs*. 0.6 mg/kg; iv qd x 1), two different doses of the non-binding control ADC B12-SG3249 (0.3 mg/kg *vs*. 0.6 mg/kg; iv qd x 1) (*Online Supplementary Figure S15*), or two different

Table 3. Loncastuximab tesirine-containing combinations in diffuse large B-cell lymphoma and mantle cell lymphoma cell lines.

Combination partner	Histology	Cell line	Median Chou-Talalay combination index	95% confidence interval
Venetoclax	ABC DLBCL	OCI-Ly-3	0.48	0.3-0.6
	ABC DLBCL	TMD8	0.63	0.48-1.17
	GCB DLBCL	VAL	0.75	0.66-0.91
	GCB DLBCL	WSU-DLCL2	0.4	0.19-1.86
	MCL	JVM2	0.37	0.25-0.69
	MCL	JEKO-1	0.88	0.37-1.01
Copanlisib	ABC DLBCL	OCI-Ly-3	0.53	0.41-0.68
	ABC DLBCL	TMD8	1.07	0.52-1.22
	GCB DLBCL	VAL	0.84	0.63-0.93
	GCB DLBCL	WSU-DLCL2	1.56	0.87-1.80
	MCL	JVM2	0.19	0.09-0.47
	MCL	JEKO-1	0.75	0.41-1.05
Idelalisib	ABC DLBCL	OCI-Ly-3	0.1	0.07-0.22
	ABC DLBCL	TMD8	0.9	0.41-1.24
	GCB DLBCL	VAL	0.86	0.67-1.22
	GCB DLBCL	WSU-DLCL2	0.5	0.30-0.75
	MCL	JVM2	0.42	0.36-0.79
	MCL	JEKO-1	1.32	0.68-1.65
Bendamustine	ABC DLBCL	OCI-Ly-3	1	0.7-1.75
	ABC DLBCL	TMD8	0.6	0.35-1.92
	GCB DLBCL	VAL	0.89	0.59-1.14
	GCB DLBCL	WSU-DLCL2	0.62	0.51-0.83
Bortezomib	ABC DLBCL	OCI-Ly-3	>3	>3
	ABC DLBCL	TMD8	1.13	0.86-1.57
Ibrutinib	ABC DLBCL	OCI-Ly-3	0.76	0.39-0.9
	ABC DLBCL	TMD8	1.07	0.96-1.25
Lenalidomide	ABC DLBCL	OCI-Ly-3	1.58	0.82-4.08
	ABC DLBCL	TMD8	1.88	0.93-2.36
Olaparib	ABC DLBCL	OCI-Ly-3	1.41	0.99-2.06
	ABC DLBCL	TMD8	0.95	0.41-1.29
	GCB DLBCL	VAL	0.86	0.67-1.22
	GCB DLBCL	WSU-DLCL2	0.5	0.30-0.75
Rituximab	ABC DLBCL	OCI-Ly-3	>3	>3
	ABC DLBCL	TMD8	>3	>3
	GCB DLBCL	VAL	0.09	0.06-0.14
	GCB DLBCL	WSU-DLCL2	>3	>3

ABC DLBCL: activated B-cell-like diffuse large B-cell lymphoma; GCB DLBCL: germinal center B-cell-like diffuse large B-cell lymphoma; MCL: mantle cell lymphoma.

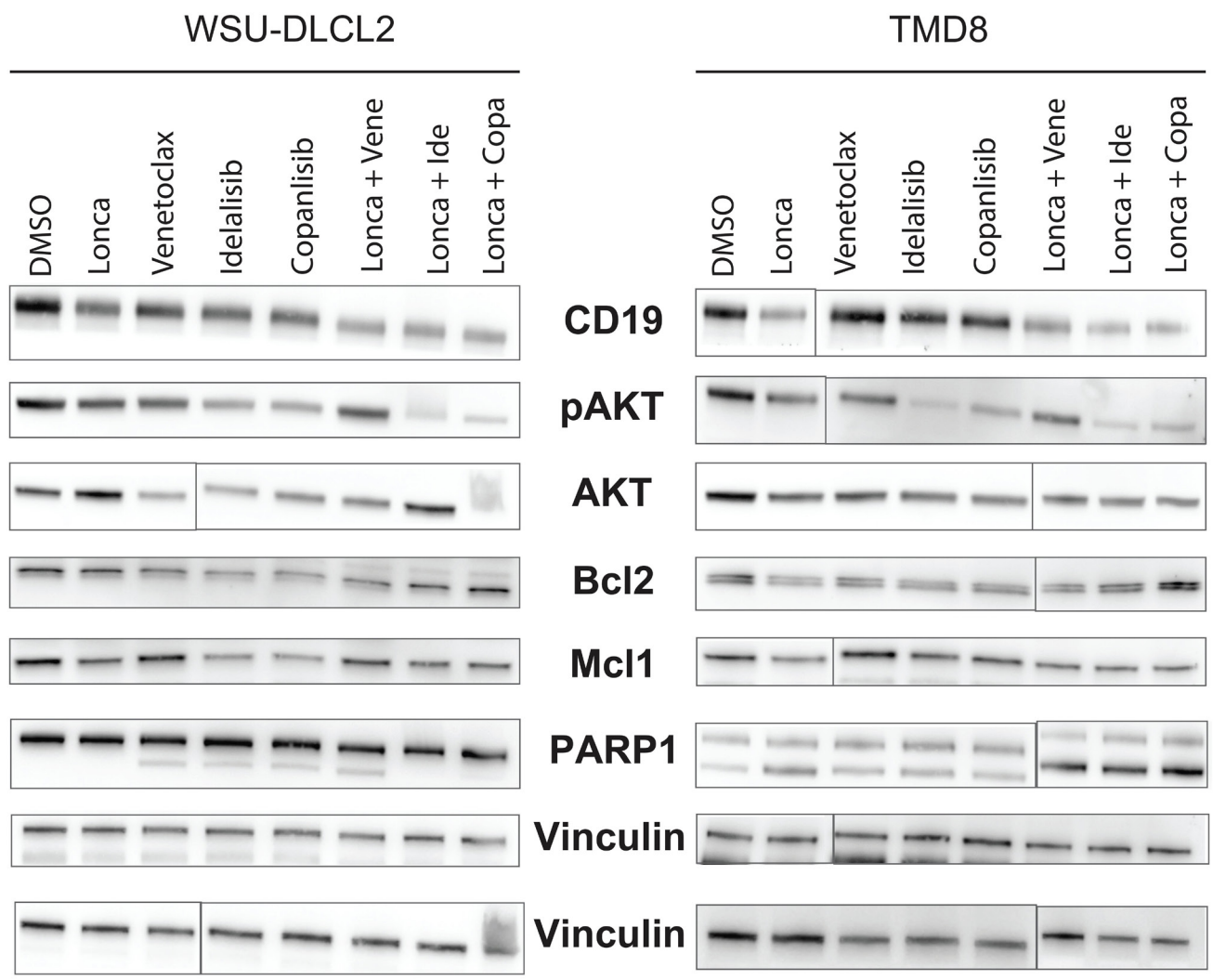

Figure 4. Proteins modulated after exposure to loncastuximab tesirine. Representative immunoblots from one germinal center B-cell-like diffuse large B-cell lymphoma cell line (WSU-DLCL2) and one activated B-cell-like diffuse large B-cell lymphoma cell line (TMD8) treated for 24 hours with drugs as single agents or with combinations of loncastuximab tesirine with venetoclax, idelalisib or copanlisib at concentrations corresponding to double the IC_{50} values. DMSO: dimethylsulfoxide; Lonca: loncastuximab tesirine; Vene: venetoclax; Ide: idelalisib; Copa: copanlisib.

schedules of copanlisib (13 mg/kg, iv; 1 day on/6 days off *vs*. 2 days on/5 days off) (*Online Supplementary Figure S16*). We defined the sub-active schedules of the drugs used in the combination study based on the observed dose-dependent antitumor activity for both loncastuximab tesirine and copanlisib. Thus, the combination experiment included animals treated with a single dose of loncastuximab tesirine (0.3 mg/kg iv; day 1; N=7) or copanlisib (13 mg/kg iv, 1 day on/6 days off; days 1 and 8; N=7) as single agents or in combination (N=9) (Figure 5A). As a control, a group of mice was treated with vehicle (phosphate-buffered saline) or non-binding control ADC B12-SG3249 at 0.3 mg/kg (N=4 each, iv, qd x 1; day 1). The combination of loncastuximab tesirine with the PIK3α/δ inhibitor copanlisib decreased tumor volume compared to that following administration of the vehicle, isotype control or single treatments (area under the curve for the combination=1.115; vehicle=3.702; B12-SG3249=2.883; copanlisib=1,952; and loncastuximab tesirine=2,032). After day 1, the antitumor effect of the combination was always superior to that of copanlisib (q<0.001), loncastuximab tesirine (q<0.001), vehicle (q<0.001), and ADC isotype control (q<0.001) treatment. The antitumor activity of B12-SG3249 did not differ from that of vehicle alone (q>0.1) or the other single-agent treatments. In terms of tumor weight, the effect of the combination was superior to that of the single agents (*P*=0.003; combination *vs*. copanlisib, *P*<0.0001; combination *vs*. loncastuximab tesirine, *P*<0.0001; combination *vs*. ADC isotype, *P*=0.003) (*Online Supplementary Figure S17A*). The combination presented an additive/slight synergistic coefficient of drug interaction (CDI) at day 38 (CDI=0.959 using B12-SG3249 as the control; CDI=1.03 using merged vehicle and B12GS3249 as the control). No toxicities were observed with single agents or combinations in this setting.

A MCL xenograft model (JEKO1) was used to assess the combination of loncastuximab tesirine with venetoclax. Mice (N=4 per group) were treated with a single injection of loncastuximab tesirine (1 mg/kg iv) and/or oral venetoclax (100 mg/kg daily 5 days a week) or vehicle at day 16 after cell injection when all tumors were palpable. Tumor volume was decreased in the animals treated with the combination arm compared to those given the vehicle and single treatments (area under the curve, combination=2,059; vehicle=4,692; venetoclax=3,470; loncastuximab tesirine=4,162), and the

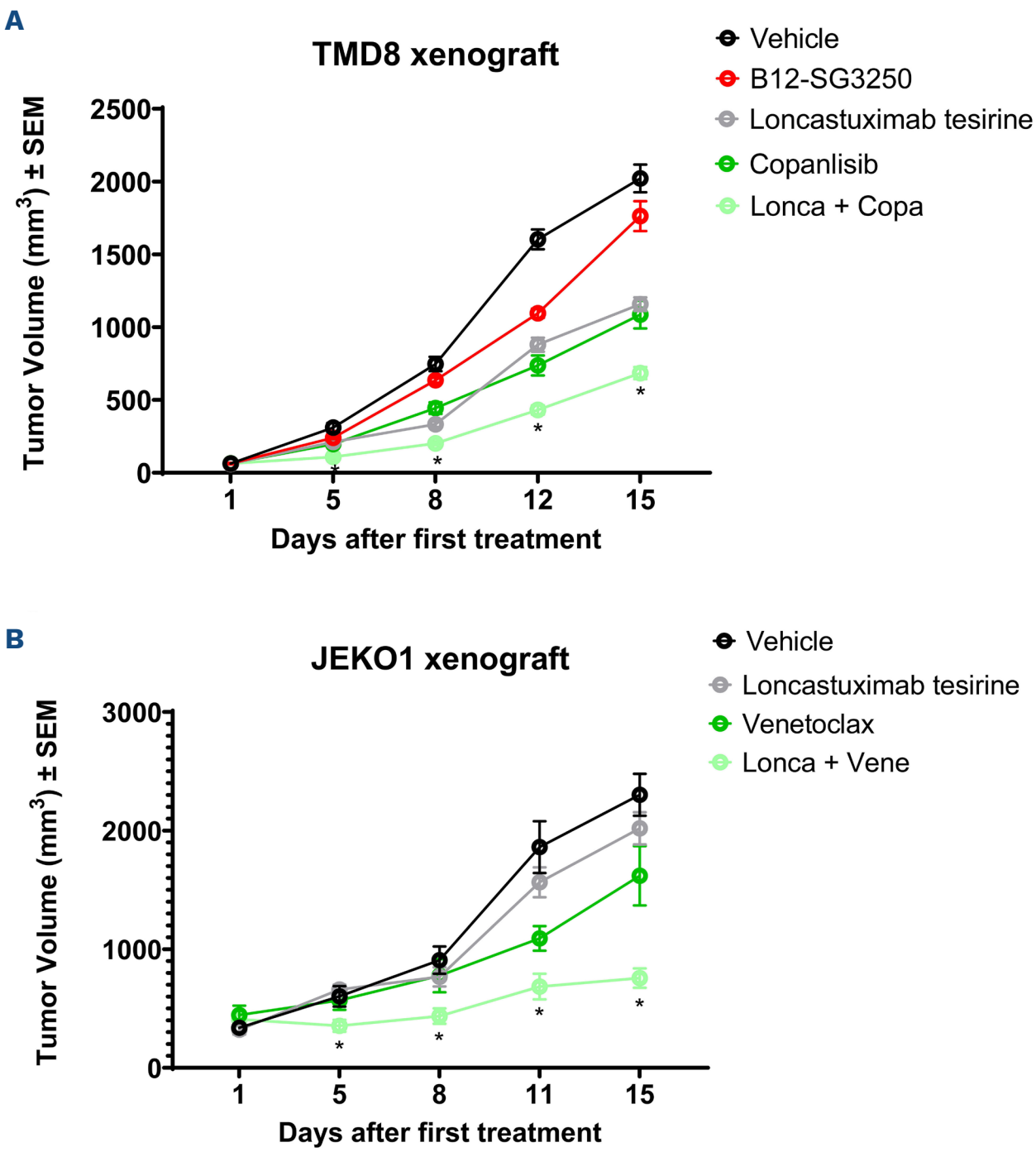

Figure 5. The combination of loncastuximab tesirine plus copanlisib or venetoclax is superior *in vivo* to single agents in activated B-cell-like diffuse large B-cell lymphoma and mantle cell lymphoma xenograft models. (A) NOD-SCID mice were subcutaneously injected with TMD8 cells and treated (N=9 per group) with loncastuximab tesirine and copanlisib as single agents and in combination and, as a control, with vehicle (phosphate-buffered saline) or the non-binding control antibody-drug conjugate B12-SG3249 (N=4 per group). *q<0.01 for the combination *versus* all other groups (vehicle, B12-SG3249, loncastuximab tesirine, copanlisib) was determined by the Mann-Whitney test followed by two-stage step-up (Benjamini, Krieger, and Yekutieli) multiple comparisons, FDR(q)=0.01. (B) NSG mice were subcutaneously injected with JEKO1 cells and treated (N=8 per group) with loncastuximab tesirine and venetoclax as single agents and in combination, and phosphate-buffered saline as a control. The average tumor volume is shown on the Y axis. *q<0.01 for the combination *versus* vehicle and loncastuximab tesirine group, as determined by the Mann-Whitney test followed by two-stage step-up (Benjamini, Krieger, and Yekutieli) multiple comparisons, FDR(q)=0.01. SEM: standard error of mean; Lonca: loncastuximab tesirine; Copa: copanlisib; Vene: venetoclax; FDR: false discovery rate.

antitumor effect was statistically significant compared to the vehicle and loncastuximab tesirine (q<0.001) as a single agent at all timepoints but day 1 (Figure 5B, *Online Supplementary Figure S17B*). A synergistic CDI (0.53) was calculated for this combination at the end of the experiment (day 15).

Discussion

In this study we have shown that: (i) the CD19-targeting ADC loncastuximab tesirine has strong cytotoxic activity in a large panel of cell lines derived from B-cell lymphomas; (ii) its *in vitro* activity correlated with the level of CD19 expression; and (iii) there is benefit of adding loncastuximab tesirine to other agents, especially BCL2 and PI3K inhibitors. We also showed the similarities and differences in activity of loncastuximab tesirine with its warhead, other CD19-targeting ADC, and R-CHOP.

These findings extend the initial preclinical data,[11] confirming loncastuximab tesirine's cytotoxic activity in mature B-cell lymphomas. In the initial publication, only a weak trend was observed between the antitumor activity of loncastuximab tesirine and CD19 expression levels across ten cell lines, including CD19-negative cells.[11] Here, we expanded the number of cell lines analyzed and, even when focusing only on B-cell lymphoma models, we observed a significant correlation between the activity of loncastuximab tesirine and CD19 expression on the cell surface as well as CD19 RNA levels, determined using multiple platforms, including one specifically designed for the analysis of formalin-fixed, paraffin-embedded clinical specimens.[29] So far, immunohistochemistry applied to tumor samples from the loncastuximab tesirine phase I and phase II trials have not demonstrated a correlation between CD19 expression and overall response rate, with patients with extremely low or no detectable immunohistochemically determined CD19 expression responding to loncastuximab tesirine.[17,30] However, our data in cell lines and the observation that measuring CD19 surface density in addition to the immunohis-

tochemically determined expression improves the response prediction[30] suggest that more sensitive measurements of CD19 in clinical specimens might be helpful to predict the type and the duration of response of patients treated with loncastuximab tesirine.

Besides loncastuximab tesirine, we tested its warhead, SG3199, on all the cell lines. As expected, SG3199 did not correlate with CD19 expression, and it was equally active in CD19-positive and CD19-negative cell lines. Interestingly, the antitumor activity of loncastuximab tesirine correlated with the intrinsic sensitivity of the cell lines to SG3199. Indeed, we could identify three different groups of cell lines. One group of cell lines was highly sensitive to both loncastuximab tesirine and SG3199 and presented the highest CD19 expression. A second group of cell lines was sensitive to the warhead but not to the ADC (IC_{50} values higher than the 75th percentile). These included models not derived from human B-cell lymphomas but also from B-cell lymphomas with low CD19 expression. One example was the VL51 cell line, derived from a splenic marginal zone lymphoma. Interestingly, we recently reported that VL51 derivatives with resistance to PI3K and BTK inhibitors, acquired after months of exposure to idelalisib or ibrutinib, present higher CD19 expression levels than the parental cells and an increased sensitivity to loncastuximab tesirine[31] and anti-CD19 CAR T cells,[32] further indicating the importance of CD19 expression levels. A third group of cell lines was characterized by IC_{50} values for both SG3199 and loncastuximab tesirine higher than the 75th percentiles, indicative of low sensitivity to the agents and intrinsic resistance to the PBD warhead.

There was no effect of histology, DLBCL cell of origin, *TP53* or *BCL2* genes status on the *in vitro* cytotoxic activity of loncastuximab tesirine. Among DLBCL cell line models, we discovered an association between *MYC* translocation, as a single alteration or together with *BCL2* translocation, and a greater sensitivity to loncastuximab tesirine and its warhead, which might be sustained by the interplay between MYC-induced replication stress and the SG3199-induced DNA interstrand cross-links.[33-35] The clinical relevance of this finding remains to be determined. Interestingly, in the phase II study, patients with *MYC* translocation were as sensitive as the remaining patients. This suggests that even this group of patients with an otherwise poor outcome can benefit from the ADC.[36]

The cytotoxic activity of PBD dimers can occur via TP53-independent and TP53-dependent mechanisms,[34] and we observed decreased activity of SG3199 in *TP53*-inactive DLBCL cell lines when compared with its activity in the *TP53* wild-type models. Although this difference was not observed when cells were exposed to loncastuximab tesirine, it suggests that payloads with an alternative mechanism of action might work better in the context of inactive *TP53*.

Next, we compared the activity of loncastuximab tesirine against all cell lines with the activity of R-CHOP, which is used in the first-line treatment of DLBCL. Loncastuximab tesirine was more active in many cell lines with low/moderate sensitivity to R-CHOP, although the antitumor activity of loncastuximab tesirine and its warhead correlated significantly with the activity of R-CHOP. Indeed, there were cell lines that were very sensitive to all treatments and, conversely, cell lines resistant to R-CHOP, loncastuximab tesirine and its warhead.

We took advantage of a previous study[28] and compared the activity of loncastuximab tesirine to that of coltuximab ravtansine and huB4-DGN462, two other CD19-targeting ADC that were analyzed using the same panel of cell lines. Interestingly, despite a higher potency, the cytotoxic activity of loncastuximab tesirine correlated with the activities of both coltuximab ravtansine and huB4-DGN462. The correlation was stronger with the latter ADC, which is more potent *in vitro* and *in vivo* than coltuximab ravtansine,[28] and carries the DNA-alkylating agent indolinobenzodiazepine pseudodimer DGN462 as its warhead,[28] rather than the maytansinoid microtubule disruptor N2'-deacetyl-N2'-(4-mercapto-4-methyl-1-oxopentyl) (DM4 or ravtansine),[37] present in coltuximab ravtansine. This observation and the comparison with R-CHOP highlight the importance of finding novel treatment modalities, including new active molecules as payloads.

We combined loncastuximab tesirine with other antilymphoma agents to identify potentially active combinations that may provide better outcomes for patients. In DLBCL, the loncastuximab tesirine-based combinations that were synergistic in most cell lines included those with the BCL2 inhibitor venetoclax, PI3K inhibitors (idelalisib, copanlisib), and with the chemotherapy agent bendamustine, followed to a lesser extent by the PARP inhibitor olaparib, the BTK inhibitor ibrutinib and the anti-CD20 monoclonal antibody rituximab. The *in vitro* findings with venetoclax and the PI3K inhibitors were extended to MCL cell lines and confirmed *in vivo*. While venetoclax has been extensively combined with small molecules, much less information regarding the combination with ADC is available. Synergy with venetoclax has been previously reported for two ADC bearing microtubule-targeting agents as payloads, the CD79B-targeting polatuzumab vedotin and the CD205-targeting MEN1309. Exposure to both agents, containing MMAE and DM4, respectively, caused downregulation of MCL1[38,39] due to protein degradation via the ubiquitin/proteasome system.[38] Also, alkylating agents have been shown to induce proteasome-mediated degradation of MCL1;[40] hence, we anticipate a similar mechanism of action mediated by loncastuximab tesirine via its SG3199 payload, supporting the observed synergism with venetoclax. The combination of loncastuximab tesirine and venetoclax is currently being explored in a phase I study (NCT05053659). No trial is being conducted to examine the combination of loncastuximab tesirine with PI3K inhibitors, which appears promising based on the *in vitro* and *in vivo* antitumor activity. The novel, highly specific PI3Kδ inhibitors seem to have an improved toxicity profile,[41,42] which might

overcome the problems observed with first-generation compounds.[43]

The combination of loncastuximab tesirine with ibrutinib, supported by other preclinical work,[44] has been clinically evaluated with results reported in R/R DLBCL and or MCL.[45] The toxicity was manageable, and the overall response rates were 67% in non-GCB DLBCL, 20% in GCB DLBCL, and 86% in MCL.[45]

The benefit of combining loncastuximab tesirine with a PARP inhibitor could lead to novel clinical opportunities. The observed benefit of combining a PBD-based ADC with a PARP inhibitor aligns with the data reported mainly in BRCA-deficient solid tumor models.[46-48] Interestingly, the GCB DLBCL marker LMO2 inhibits BRCA1 recruitment to DNA double-strand breaks in DLBCL cells, causing a BRCA1-deficiency-like phenotype and sensitizing DLBCL cells to PARP inhibition.[49] Indeed, we observed synergism in the GCB DLBCL cells but only an additive effect in one of the two ABC DLBCL models. PARP inhibitors have been explored in lymphoma patients.[50] In particular, the PARP inhibitor veliparib has shown evidence of clinical activity, including complete remissions and safety in combination with bendamustine with or without rituximab.[50,51]

Since there are multiple CD19-targeting therapeutic modalities that share CD19 loss as one of the mechanisms of resistance,[4,6-10,52] it will be crucial to define the best sequencing or prioritization strategy for using these agents,[53-57] as well as their integration with bispecific antibodies.[6-8] Here, we demonstrated the *in vitro* activity of loncastuximab tesirine in a cell line derived from a patient who progressed after CD19-targeting CAR T-cell therapy, strengthening the clinical data showing responses in patients after treatment with CAR T cells.[53,57]

In conclusion, our data support the further development of loncastuximab tesirine as a single agent and in combination for patients affected by mature B-cell neoplasms. The results also highlight the importance of CD19 expression and the existence of lymphoma populations characterized by resistance to multiple therapies.

Disclosures

CT has received a travel grant from iOnctura. LC has received a travel grant from HTG Molecular Diagnostics. EZ has been a member of advisory boards for BeiGene, BMS, Curis, Eli/Lilly, Incyte, Janssen, Merck, Miltenyi Biomedicine, and Roche; has received research support from AstraZeneca, Beigene, BMS/Celgene, Incyte, Janssen, and Roche; and has received travel grants from BeiGene, Janssen, Gilead, and Roche. AS has sat on advisory boards for Janssen and Roche; has received research funding from AbbVie, ADC Therapeutics, Amgen, AstraZeneca, Bayer, Cellestia, Incyte, LoxoOncology, Merck MSD, Novartis, Pfizer, Philogen, and Roche; has received a travel grant from AstraZeneca; and has provided expert testimony for Bayer and Eli Lilly. DR has received honoraria from AstraZeneca, AbbVie, BeiGene, BMS/Celgene, and Janssen and has received research funding from AstraZeneca, AbbVie, BeiGene, and Janssen. PHvB and FZ are employed by ADC Therapeutics and own stocks in the company. PFC has received research funding from ADC Therapeutics, grants from Genentech, and advisory board consultancy fees from ADC Therapeutics, Novartis, BMS, Genentech, and SOBI. FB has received institutional research funds from ADC Therapeutics, Bayer AG, BeiGene, Helsinn, HTG Molecular Diagnostics, Ideogen AG, Idorsia Pharmaceuticals Ltd., Immagene, ImmunoGen, Menarini Ricerche, Nordic Nanovector ASA, Oncternal Therapeutics, and Spexis AG; has received consultancy fees from BIMINI Biotech, Helsinn, and Menarini; has received advisory board fees for his institution from Novartis; has provided expert statements to HTG Molecular Diagnostics; and has received travel grants from Amgen, Astra Zeneca, and iOnctura. The other authors have no conflicts of interest to disclose.

Contributions

CT performed experiments and data mining, interpreted data and co-wrote the manuscript. FS and EG performed experiments and interpreted data. LC performed data mining. DW, EC, AJA, GG, LS, MTC, and GI performed experiments. NM and AB performed experiments and data mining. AB and DR performed targeted DNA sequencing and data mining. EZ and AS provided advice. PHvB and FZ co-designed the study, provided reagents, and supervised the study. FB co-designed the study, performed data mining, interpreted data, supervised the study, and co-wrote the manuscript. All authors reviewed and accepted the final version of the manuscript.

Acknowledgments

We thank our colleagues Dr Antonella Zucchetto and Dr Valter Gattei (Aviano, Italy) for their helpful discussion.

Funding

This project was partially supported by research funds from ADC Therapeutics, the Swiss National Science Foundation grant SNSF 310030_197466, the Swiss Cancer Research grant KFS-4713-02-2019 (to FB), LLS 7027-23, and LLS-SCOR 7026-21 (to GI). NM was supported by a Ph.D. Fellowship of the NCCR RNA & Disease, a National Center of Competence in Research funded by the Swiss National Science Foundation (grant numbers 182880 and 205601).

Data-sharing statement

All data are included in the manuscript and in the Online Supplementary Material.

References

1. Roser M, Ritchie H. Cancer. 2019. https://ourworldindata.org/cancer. Accessed November 1, 2023.
2. Sung H, Ferlay J, Siegel RL, et al. Global cancer statistics 2020: GLOBOCAN estimates of incidence and mortality worldwide for 36 cancers in 185 countries. CA Cancer J Clin. 2021;71(3):209-249.
3. Sehn LH, Salles G. Diffuse large B-cell lymphoma. N Engl J Med. 2021;384(9):842-858.
4. Barreca M, Lang N, Tarantelli C, Spriano F, Barraja P, Bertoni F. Antibody-drug conjugates for lymphoma patients: preclinical and clinical evidences. Explor Target Antitumor Ther. 2022;3(6):763-794.
5. Dumontet C, Reichert JM, Senter PD, Lambert JM, Beck A. Antibody-drug conjugates come of age in oncology. Nat Rev Drug Discov. 2023;22(8):641-661.
6. Abramson JS, Ghosh N, Smith SM. ADCs, BiTEs, CARs, and small molecules: a new era of targeted therapy in non-Hodgkin lymphoma. Am Soc Clin Oncol Educ Book. 2020;40:302-313.
7. de Ramon Ortiz C, Wang S, Stathis A, et al. How to integrate CD19 specific chimeric antigen receptor T cells with other CD19 targeting agents in diffuse large B-cell lymphoma? Hematol Oncol. 2024;42(1):e3237.
8. Sermer D, Elavalakanar P, Abramson JS, Palomba ML, Salles G, Arnason J. Targeting CD19 for diffuse large B cell lymphoma in the era of CARs: other modes of transportation. Blood Rev. 2023;57:101002.
9. Bailly S, Cartron G, Chaganti S, et al. Targeting CD19 in diffuse large B-cell lymphoma: an expert opinion paper. Hematol Oncol. 2022;40(4):505-517.
10. Varma G, Goldstein J, Advani RH. Novel agents in relapsed/refractory diffuse large B-cell lymphoma. Hematol Oncol. 2023;41(Suppl 1):92-106.
11. Zammarchi F, Corbett S, Adams L, et al. ADCT-402, a PBD dimer-containing antibody drug conjugate targeting CD19-expressing malignancies. Blood. 2018;131(10):1094-1105.
12. Francisco JA, Cerveny CG, Meyer DL, et al. cAC10-vcMMAE, an anti-CD30-monomethyl auristatin E conjugate with potent and selective antitumor activity. Blood. 2003;102(4):1458-1465.
13. Dornan D, Bennett F, Chen Y, et al. Therapeutic potential of an anti-CD79b antibody-drug conjugate, anti-CD79b-vc-MMAE, for the treatment of non-Hodgkin lymphoma. Blood. 2009;114(13):2721-2729.
14. Antonow D, Thurston DE. Synthesis of DNA-interactive pyrrolo[2,1-c][1,4]benzodiazepines (PBDs). Chem Rev. 2011;111(4):2815-2864.
15. Hartley JA, Flynn MJ, Bingham JP, et al. Pre-clinical pharmacology and mechanism of action of SG3199, the pyrrolobenzodiazepine (PBD) dimer warhead component of antibody-drug conjugate (ADC) payload tesirine. Sci Rep. 2018;8(1):10479.
16. Caimi PF, Ai W, Alderuccio JP, et al. Loncastuximab tesirine in relapsed or refractory diffuse large B-cell lymphoma (LOTIS-2): a multicentre, open-label, single-arm, phase 2 trial. Lancet Oncol. 2021;22(6):790-800.
17. Hamadani M, Radford J, Carlo-Stella C, et al. Final results of a phase 1 study of loncastuximab tesirine in relapsed/refractory B-cell non-Hodgkin lymphoma. Blood. 2021;137(19):2634-2645.
18. Jain N, Stock W, Zeidan A, et al. Loncastuximab tesirine, an anti-CD19 antibody-drug conjugate, in relapsed/refractory B-cell acute lymphoblastic leukemia. Blood Adv. 2020;4(3):449-457.
19. Caimi PF, Ai WZ, Alderuccio JP, et al. Loncastuximab tesirine in relapsed/refractory diffuse large B-cell lymphoma: long-term efficacy and safety from the phase II LOTIS-2 study. Haematologica. 2024;109(4):1184-1193.
20. Calabretta E, Hamadani M, Zinzani PL, Caimi P, Carlo-Stella C. The antibody-drug conjugate loncastuximab tesirine for the treatment of diffuse large B-cell lymphoma. Blood. 2022;140(4):303-308.
21. Boi M, Gaudio E, Bonetti P, et al. The BET bromodomain inhibitor OTX015 affects pathogenetic pathways in preclinical B-cell tumor models and synergizes with targeted drugs. Clin Cancer Res. 2015;21(7):1628-1638.
22. Golay J, Semenzato G, Rambaldi A, et al. Lessons for the clinic from rituximab pharmacokinetics and pharmacodynamics. MAbs. 2013;5(6):826-837.
23. Habermann TM, Weller EA, Morrison VA, et al. Rituximab-CHOP versus CHOP alone or with maintenance rituximab in older patients with diffuse large B-cell lymphoma. J Clin Oncol. 2006;24(19):3121-3127.
24. de Jong MRW, Langendonk M, Reitsma B, et al. Heterogeneous pattern of dependence on anti-apoptotic BCL-2 family proteins upon CHOP treatment in diffuse large B-cell lymphoma. Int J Mol Sci. 2019;20(23):6036.
25. Spriano F, Tarantelli C, Cascione L, et al. Targeting CD25-positive lymphoma cells with the antibody-drug conjugate camidanlumab tesirine as single agent or in combination with targeted agents. bioRxiv. 2023 July 2. doi: 10.1101/2023.07.02.547392 [preprint, not peer-reviewed].
26. Tarantelli C, Gaudio E, Arribas AJ, et al. PQR309 is a novel dual PI3K/mTOR inhibitor with preclinical antitumor activity in lymphomas as a single agent and in combination therapy. Clin Cancer Res. 2018;24(1):120-129.
27. Johnson Z, Tarantelli C, Civanelli E, et al. IOA-244 is a non-ATP-competitive, highly selective, tolerable PI3K delta inhibitor that targets solid tumors and breaks immune tolerance. Cancer Res Commun. 2023;3(4):576-591.
28. Hicks SW, Tarantelli C, Wilhem A, et al. The novel CD19-targeting antibody-drug conjugate huB4-DGN462 shows improved anti-tumor activity compared to SAR3419 in CD19-positive lymphoma and leukemia models. Haematologica. 2019;104(8):1633-1639.
29. Ran D, Moharil J, Lu J, et al. Platform comparison of HTG EdgeSeq and RNA-Seq for gene expression profiling of tumor tissue specimens. J Clin Oncol. 2020;38(15):3566.
30. Caimi PF, Hamadani M, Carlo-Stella C, et al. In relapsed or refractory diffuse large B-cell lymphoma, CD19 expression by immunohistochemistry alone is not a predictor of response to loncastuximab tesirine. EJHaem. 2024;5(1):76-83.
31. Arribas AJ, Napoli S, Cascione L, et al. Resistance to PI3κδ inhibitors in marginal zone lymphoma can be reverted by targeting the IL-6/PDGFRA axis. Haematologica. 2022;107(11):2685-2697.
32. Wang SS, Arribas AJ, Tarantelli C, et al. PI3K and BTK inhibition induces the upregulation of CD19 and increases sensitivity to CAR T cells in a model of marginal zone lymphoma (MZL). Blood. 2022;140(Supplement 1):4554-4555.
33. Curti L, Campaner S. MYC-induced replicative stress: a double-edged sword for cancer development and treatment. Int J Mol Sci. 2021;22(12):6168.

34. Mantaj J, Jackson PJ, Rahman KM, Thurston DE. From anthramycin to pyrrolobenzodiazepine (PBD)-containing antibody-drug conjugates (ADCs). Angew Chem Int Ed Engl. 2017;56(2):462-488.
35. Mao S, Chaerkady R, Yu W, et al. Resistance to pyrrolobenzodiazepine dimers is associated with SLFN11 downregulation and can be reversed through inhibition of ATR. Mol Cancer Ther. 2021;20(3):541-552.
36. Alderuccio JP, Ai WZ, Radford J, et al. Loncastuximab tesirine in relapsed/refractory high-grade B-cell lymphoma: a subgroup analysis from the LOTIS-2 study. Blood Adv. 2022;6(16):4736-4739.
37. Blanc V, Bousseau A, Caron A, Carrez C, Lutz RJ, Lambert JM. SAR3419: an anti-CD19-maytansinoid immunoconjugate for the treatment of B-cell malignancies. Clin Cancer Res. 2011;17(20):6448-6458.
38. Amin DN, Bannerji R, Mali RS, et al. Abstract CT133: Targeting BCL-2 and MCL-1 overcomes treatment resistance in relapsed and refractory non-Hodgkin lymphoma: pre-clinical rationale and results from an open-label phase 1b study. Cancer Res. 2020;80(16_Supplement):CT133.
39. Gaudio E, Tarantelli C, Spriano F, et al. Targeting CD205 with the antibody drug conjugate MEN1309/OBT076 is an active new therapeutic strategy in lymphoma models. Haematologica. 2020;105(11):2584-2591.
40. Chiou JT, Huang NC, Huang CH, et al. NOXA-mediated degradation of MCL1 and BCL2L1 causes apoptosis of daunorubicin-treated human acute myeloid leukemia cells. J Cell Physiol. 2021;236(11):7356-7375.
41. Zelenetz AD, Jurczak W, Ribrag V, et al. Efficacy and safety of single-agent zandelisib administered by intermittent dosing in patients with relapsed or refractory (R/R) follicular lymphoma (FL): final results of the Tidal phase 2 study. Blood. 2022;140(Supplement 1):3595-3597.
42. Carlo-Stella C, Tarantelli C, Civanelli E, et al. Highly selective allosteric modulator of the phosphoinositide 3-kinase delta (PI3Kδ) roginolisib in patients with refractory/relapsed follicular lymphoma. Hematol Oncol. 2023;41(S2):574-574.
43. Brown JR, Danilov AV, LaCasce AS, Davids MS. PI3K inhibitors in haematological malignancies. Lancet Oncol. 2022;23(8):e364.
44. Cucchi D, Sachini N, van Berkel PH, Zammarchi F. Mechanistic studies investigating the synergistic combination of loncastuximab tesirine and ibrutinib in pre-clinical models of B-cell non-Hodgkin lymphoma. Cancer Res. 2022;82(12_Supplement):1050.
45. Depaus J, Wagner-Johnston N, Zinzani PL, et al. Clinical activity of loncastuximab tesirine plus ibrutinib in non-Hodgkin lymphoma: updated Lotis 3 phase 1 results. Hematol Oncol. 2021;39(S2):325.
46. Zhong H, Chen C, Tammali R, et al. Improved therapeutic window in BRCA-mutant tumors with antibody-linked pyrrolobenzodiazepine dimers with and without PARP inhibition. Mol Cancer Ther. 2019;18(1):89-99.
47. Zammarchi F, Havenith KE, Chivers S, et al. Preclinical development of ADCT-601, a novel pyrrolobenzodiazepine dimer-based antibody-drug conjugate targeting AXL-expressing cancers. Mol Cancer Ther. 2022;21(4):582-593.
48. Fusani S, Rossi A, Mazzara S, et al. CD19-mediated DNA damage boost in lymphoma cells treated with loncastuximab tesirine in combination with PARP inhibitors. Blood. 2021;138(Supplement 1):1342.
49. Parvin S, Ramirez-Labrada A, Aumann S, et al. LMO2 confers synthetic lethality to PARP inhibition in DLBCL. Cancer Cell. 2019;36(3):237-249.
50. Carrassa L, Colombo I, Damia G, Bertoni F. Targeting the DNA damage response for patients with lymphoma: preclinical and clinical evidences. Cancer Treat Rev. 2020;90:102090.
51. Soumerai JD, Zelenetz AD, Moskowitz CH, et al. The PARP inhibitor veliparib can be safely added to bendamustine and rituximab and has preliminary evidence of activity in B-cell lymphoma. Clin Cancer Res. 2017;23(15):4119-4126.
52. Strati P, Neelapu SS. CAR-T failure: beyond antigen loss and T cells. Blood. 2021;137(19):2567-2568.
53. Caimi PF, Ardeshna KM, Reid E, et al. The antiCD19 antibody drug immunoconjugate loncastuximab achieves responses in DLBCL relapsing after AntiCD19 CAR-T cell therapy. Clin Lymphoma Myeloma Leuk. 2022;22(5):e335-e339.
54. Horvei P, Sakemura R, Cox MJ, et al. Targeting of CD19 by tafasitamab does not impair CD19 directed chimeric antigen receptor T cell activity in vitro. Biol Blood Marrow Transplant. 2020;26(3):S223-S224.
55. Tabbara N, Gaut D, Oliai C, Lewis T, de Vos S. Anti-CD19 CAR T-cell therapy remission despite prior anti-CD19 antibody tafasitamab in relapsed/refractory DLBCL. Leuk Res Rep. 2021;16:100260.
56. Thapa B, Caimi PF, Ardeshna KM, et al. CD19 antibody-drug conjugate therapy in DLBCL does not preclude subsequent responses to CD19-directed CAR T-cell therapy. Blood Adv. 2020;4(16):3850-3852.
57. Dodero A, Bramanti S, Di Trani M, et al. Outcome after chimeric antigen receptor (CAR) T-cell therapy failure in large B-cell lymphomas. Br J Haematol. 2024;204(1):151-159.